Bromine-Loss and Hydrogen-Loss Dissociations in Low-Lying Electronic States of the CH_3Br^+ Ion Studied Using Multiconfiguration Second-Order Perturbation Theory

Hong-Wei Xi and Ming-Bao Huang*

College of Chemistry and Chemical Engineering, Graduate University, Chinese Academy of Sciences, P.O. Box 4588, Beijing 100049, People's Republic of China

Received: October 25, 2005; In Final Form: January 4, 2006

Complete active space self-consistent field (CASSCF) and multiconfiguration second-order perturbation theory (CASPT2) calculations with an ANO−RCC basis were performed for the $1^2A'$, $1^2A''$, $2^2A'$, and $2^2A''$ states of the CH_3Br^+ ion. The $1^2A'$ state is predicted to be the ground state. The $2^2A'$ state is predicted to be a bound state. The adiabatic and vertical excitation energies and the relative energies at the molecular geometry were calculated, and the energetic results for $2^2A'$ and $2^2A''$ are in reasonable agreement with the experimental data. Potential energy curves (PECs) for Br-loss and H-loss dissociations from the four C_s states were calculated at the CASPT2//CASSCF level and the electronic states of the CH_3^+ and CH_2Br^+ ions as the dissociation products were determined by checking the relative energies and geometries of the asymptote products along the PECs. In the Br-loss dissociation, the $1^2A'$, $1^2A''$, and $2^2A'$ states correlate with CH_3^+ (X^1A_1') and the $2^2A''$ state correlates with CH_3^+ ($1^3A''$). The energy increases monotonically with the R(C−Br) value along the four Br-loss PECs. In the H-loss dissociation the $1^2A'$, $1^2A''$, $2^2A'$, and $2^2A''$ states correlate with the X^1A_1, $1^3A''$, $1^3A'$, and $1^1A''$ states ($1^3A'$ lying above $1^1A''$) of CH_2Br^+, respectively. Along the $2^2A''$ H-loss PEC there is an energy barrier and the CASSCF wave functions at large R(C−H) values have shake-up ionization character. Along the $2^2A'$ H-loss PEC there are an energy barrier and a minimum. At the end of the present paper we present a comprehensive review on the electronic states and the X-loss and H-loss dissociations of the CH_3X^+ (X = F, Cl, and Br) ions on the basis of our previous studies and the present study.

I. Introduction

During the past three decades, numerous experimental studies were reported on dissociation of the halogenated methane ions (CH_3X^+; X = F, Cl, and Br) from their low-lying electronic states. The experimental studies[1−7] on the CH_3Br^+ ion were relatively few, compared to those on the CH_3F^+ and CH_3Cl^+ ions. In 1976, Eland et al.[1] mapped out a general picture for dissociation of the CH_3X^+ ions from the X, A, and B states on the basis of their photoelectron-photoion coincidence experiments. In 1993 Lane and Powis[2] reported their experimental study on dissociation of the CH_3Br^+ ion from the X and A states. Since 2000, Locht's group[8−12] investigated in detail the photoabsorption and photoionization dynamics of CH_3X (X = F, Cl, and Br) by using vacuum UV photoabsoption spectrum, and the two lowest-lying C_s states (see below) of the CH_3X^+ ions were studied. To examine the experimentally suggested schemes of the pathways for X-loss and H-loss dissociations from the low-lying electronic states of the CH_3F^+ and CH_3Cl^+ ions, we carried out theoretical studies[13,14] using the CASSCF (complete active space self-consistent field)[15] and CASPT2 (multiconfiguration second-order perturbation theory)[16,17] methods. In the present work we have carried out theoretical study on Br-loss and H-loss dissociations from low-lying electronic states of the CH_3Br^+ ion using the CASSCF and CASPT2 methods.

In the previous experimental studies the X^2E, A^2A_1, and B^2E states were considered to be the three lowest-lying electronic states of the CH_3X^+ ions. Because of the Jahn−Teller effect in the degenerate ^2E states, the three lowest-lying C_{3v} states of the CH_3X^+ ions become the five lowest-lying C_s states: $1^2A''$, $1^2A'$, $2^2A'$ (A^2A_1), $2^2A''$, and $3^2A'$. In theoretical studies on X-loss and H-loss dissociations of the CH_3X^+ ions one should explicitly consider the C_s states of the CH_3X^+ reaction systems (one should also explicitly give electronic states of the CH_3^+ and CH_2X^+ ions as the products of dissociation from the different C_s states of the CH_3X^+ ions). In the present work we have studied Br-loss and H-loss dissociations of the CH_3Br^+ ion from the $1^2A'$, $1^2A''$, $2^2A'$, and $2^2A''$ states. To the best of our knowledge, there are no reported theoretical studies on electronic states of the CH_3Br^+ ion in the literature, except the study[18] of Lugez et al. on the $1^2A'$ state and the study[8] of Locht et al. on the $1^2A'$ and $1^2A''$ states. In the present article we will first briefly report the calculated equilibrium geometries and energetics for the four C_s states and then describe and discuss the calculated reaction paths for Br-loss and H-loss dissociations from the four states. In the conclusion section of the present article we will present a comprehensive review of our CAS (CASSCF and CASPT2) theoretical studies on the CH_3F^+,[13] CH_3Cl^+,[14] and CH_3Br^+ ions.

II. Calculation Details

Geometry and atom labelings used for the CH_3Br^+ ion (C_s symmetry) are shown in Figure 1, and the H_1 atom in the symmetry plane is assumed to be the leaving species in H-loss dissociation. The CAS (CASSCF and CASPT2) calculations were carried out using the *MOLCAS* v5.4 quantum-chemistry software.[19] With a CASSCF wave function constituting the

* Corresponding author. E-mail: mbhuang1@gucas.ac.cn.

10.1021/jp056138r CCC: $33.50
Published on Web 06/13/2006

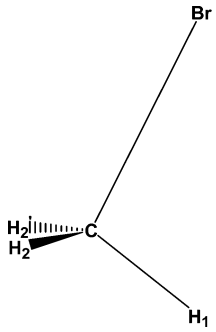

Figure 1. Atom labelings in the bromomethane ion used in the present study.

reference function the CASPT2 calculations were performed to compute the first-order wave function and the second-order energy in the full-CI space. In our previous CAS studies[13,14] for the CH_3F^+ and CH_3Cl^+ ions we used the contracted atomic natural orbital basis ANO-L.[20−22] Considering that the CH_3Br^+ ion contains a heavy atom we used an ANO−RCC basis,[21,23] Br[6s5p3d2f1 g]/C[4s3p2d1f]/H[3s2p1d], in the CAS calculations of the present work. The ANO−RCC basis sets[21,23] were constructed to include scalar relativistic effects (using the Douglas−Kroll Hamiltonian) and correlation of the outermost core electrons.

The CASSCF geometry optimization and frequency calculations were performed for the $1^2A'$, $1^2A''$, $2^2A'$, and $2^2A''$ states (the calculations for $3^2A'$ were not successful). On the basis of the CASPT2 calculations at the CASSCF optimized geometries, we obtained the CASPT2//CASSCF adiabatic excitation energies (T_0's) for the excited states ($1^2A'$ being predicted to be the ground state). On the basis of the CASPT2 calculations at the CASSCF geometry of the $1^2A'$ state, we obtained the CASPT2//CASSCF vertical excitation energies (T_v's) for the excited states. The "CASPT2//CASSCF T_0 values" and "CASPT2//CASSCF T_v values" will be abbreviated to "CASPT2 T_0 values" and "CASPT2 T_v values", respectively. On the basis of the CASPT2 calculations for the four states at the experimental geometry[24] of the ground-state CH_3Br molecule (abbreviated to "experimental molecular geometry"), we obtained the CASPT2 relative energies (denoted as CASPT2 T_v''s) of the four states to the $1^2A'$ state.

In the calculations of potential energy curves (PECs) for Br-loss dissociation from the $1^2A'$, $1^2A''$, $2^2A'$, and $2^2A''$ states of CH_3Br^+, the C−Br distance [R(C−Br)] was taken as the reaction coordinate. At a set of fixed R(C−Br) values (10 or more values) ranging from the C−Br bond length values in the CASSCF optimized geometries of the respective states (from 2.3 Å for $2^2A'$; see below) to 5.0 Å we performed the CASSCF partial geometry optimization calculations followed by the CASPT2 energy calculations at the four sets of the partially optimized geometries, and we obtained the four CASPT2//CASSCF Br-loss dissociation PECs (abbreviated to "Br-loss PECs") (see section III.B for the technical treatments in the Br-loss PEC calculations for $1^2A'$). In the calculations of PECs for H-loss dissociation from the $1^2A'$, $1^2A''$, $2^2A'$, and $2^2A''$ states of CH_3Br^+, the C−H_1 distance [R(C−H_1)] was taken as the reaction coordinate. At a set of fixed R(C−H_1) values (12 or more values) ranging from the C−H_1 bond length values in the CASSCF optimized geometries of the respective states to 5.0 Å (to 8.0 Å for $2^2A'$; see below) we performed the CASSCF partial geometry optimization calculations followed by the CASPT2 energy calculations, and we obtained the four CASPT2//CASSCF H-loss dissociation PECs (abbreviated to "H-loss PECs").

In the CASSCF calculations, we used the full-valence active space, which includes eight a′ (12a′-19a′) and three a″ (5a″-7a″) orbitals (13 electrons and 11 active orbitals). In the CASPT2 calculations, the weight values of the CASSCF reference functions in the first-order wave functions were all larger than 0.83.

III. Results and Discussion

A. Geometries and Excitation Energies. In Table 1 are given the CASSCF optimized geometries for the $1^2A'$, $1^2A''$, $2^2A'$, and $2^2A''$ states. The CASSCF frequency calculations predict that the $1^2A''$ and $2^2A''$ states have unique imaginary frequencies (see Table 1). The vibration modes associated with these imaginary frequencies describe pivotal motion of the three hydrogen atoms, and therefore, these imaginary frequencies are not related to transition states (if any) in Br-loss or H-loss dissociation reactions of the $1^2A''$ and $2^2A''$ states. In Table 2 are given the CASPT2 T_0 values for the $1^2A'$ and $2^2A'$ states and the CASPT2 T_v and T_v' values for the $1^2A'$, $1^2A''$, $2^2A'$, and $2^2A''$ states. These energetic calculations indicate that $1^2A'$ is the ground state of the CH_3Br^+ ion. On the basis of their photoelectron spectra, Karlsson et al.[25] reported adiabatic ionization potential (AIP) values of 10.543, 13.0, and 14.5 eV for the X^2E, A^2A_1, and B^2E states of CH_3Br^+, respectively, and they also reported vertical ionization potential (VIP) values of 10.543 and 13.5 eV for the X^2E and A^2A_1 states, respectively, and two VIP values of 15.0 and 15.7 eV for the B^2E state. The T_0 values for excited states of the CH_3Br^+ ion are considered to be equal to the differences between the AIP values for excited states and the AIP value for the ground state of the ion, and therefore the experimental T_0 values are 2.46 and 3.96 eV for A^2A_1 and B^2E, respectively, evaluated using the experimental AIP values.[25] The T_v' values are considered to be equal to the differences between the VIP values for excited states and the VIP value for the ground state of the ion, and therefore we have an experimental T_v' value of 2.96 eV for A^2A_1 and two experimental T_v' values of 4.46 and 5.16 eV for B^2E, evaluated using the experimental VIP values.[25] All these experimental T_0 and T_v' values are listed in Table 2.

In our previous studies[13,14] for the CH_3F^+ and CH_3Cl^+ ions we failed to obtain CASSCF optimized geometries for the $2^2A'$ states of the two ions. The experimental studies[1,26−28] indicated that the $2^2A'$ (A^2A_1) states of CH_3F^+ and CH_3Cl^+ be repulsive. In the present study we obtained a CASSCF optimized geometry for the $2^2A'$ state of CH_3Br^+ and the CASSCF frequency calculations indicate that the geometry corresponds to a minimum in the $2^2A'$ potential energy surface (PES). Therefore, the $2^2A'$ (A^2A_1) state of CH_3Br^+ is not a repulsive state. The CASSCF geometry for the $2^2A'$ state of CH_3Br^+ has essentially the C_{3v} symmetry (see Table 1) and it has a very long C−Br bond length (2.630 Å) and relatively small HCBr bond angles. We reoptimized the C−Br bond length and HCBr bond angles in the $2^2A'$ (A^2A_1) geometry at the CASPT2 level [the C−H bond lengths being fixed at a value of 1.098 Å (see Table 1)], and we obtained a CASPT2 optimized C−Br bond length value of 2.315 Å, which is significantly smaller than the CASSCF value (the CASPT2 optimized HCBr bond angle values being 94.0°).

The CASPT2 T_0 value of 2.28 eV for $2^2A'$ is in reasonable agreement with the experimental T_0 value of 2.46 eV for the A^2A_1 state.[25] The CASPT2 T_v' value of 2.91 eV for $2^2A'$ is very close to the experimental T_v' value of 2.96 eV for the A^2A_1 state,[25] and the CASPT2 T_v' value of 4.84 eV for $2^2A''$ is very close to the average (4.81 eV) of the two experimental T_v' values of 4.46 and 5.16 eV for the B^2E state.[25]

TABLE 1: CASSCF Optimized Geometries for the $1^2A'$, $1^2A''$, $2^2A'$, and $2^2A''$ States of the CH_3Br^+ Ion[a]

state	R(C−Br) (Å)	R(C−H_1) (Å)	R(C−H_2) (Å)	A(H_1CBr) (deg)	A(H_2CBr) (deg)	D(H_2CBrH_2') (deg)	imaginary frequencies[b]
$1^2A'$	1.996	1.104	1.097	102.4	105.8	123.1	no
$1^2A''$	1.998	1.094	1.101	106.4	103.7	117.2	−588
$2^2A'$	2.630(2.315)[c]	1.098	1.098	92.3 (94.0)[c]	92.2 (94.0)[c]	120.0	no
$2^2A''$	2.065	1.096	1.185	114.1	115.8	84.6	−1478

[a] Bond length, bond angle, and dihedral angle are denoted as R, A, and D, respectively; for notations; see Figure 1. [b] The unique imaginary frequencies (in cm^{-1}) obtained in the CASSCF frequency calculations, and they are associated with H-pivotal rotations. [c] In parentheses are given the CASPT2 optimized values.

TABLE 2: CASPT2 Adiabatic (T_0) and Vertical (T_v) Excitation Energies for the $1^2A'$, $1^2A''$, $2^2A'$, and $2^2A''$ States of the CH_3Br^+ Ion Calculated Using the CASSCF Optimized Geometries and the CASPT2 Relative Energies (T_v') of the Four States Calculated at the Experimental Geometry[a] of the Ground-State CH_3Br Molecule

	T_0 (eV)		T_v(eV)	T_v' (eV)	
state	CASPT2	exptl[b]	CASPT2	CASPT2	exptl[c]
$1^2A'$	0.0	X^2E: 0.0	0.0	0.0	X^2E: 0.0
$1^2A''$			0.05	0.01	
$2^2A'$	2.28	A^2A_1: 2.46	2.65	2.91	A^2A_1:2.96
$2^2A''$		B^2E: 3.96	5.00	4.84	B^2E: 4.46, 5.16

[a] The experimental geometry (C_{3v}): R(C−Br) = 1.939 Å, R(C−H) = 1.095 Å, and ∠HCBr = 107.2°; see ref 24. [b] Evaluated using the experimental AIP values reported in ref 25 (the value for X^2E being 10.543 eV). [c] Evaluated using the experimental VIP values reported in ref 25 (the value for X^2E being 10.543 eV).

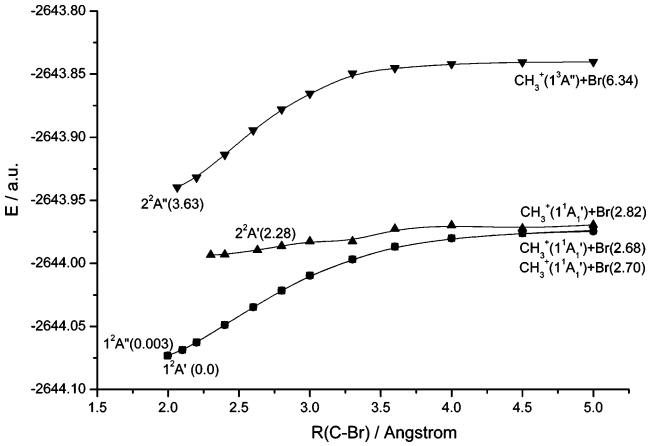

Figure 2. CASPT2//CASSCF potential energy curves (PECs) for Br-loss dissociation from the $1^2A'$, $1^2A''$, $2^2A'$, and $2^2A''$ states. In parentheses are given the CASPT2//CASSCF relative energies (in eV) of the reactants and asymptote products along the PECs to the $1^2A'$ reactant.

B. Br-Loss Dissociation. In Figure 2 are given the CASPT2//CASSCF Br-loss PECs for the $1^2A'$, $1^2A''$, $2^2A'$, and $2^2A''$ states of the CH_3Br^+ ion. The calculation procedure for the $1^2A''$, $2^2A'$, and $2^2A''$ PECs was described in section II. We will describe the calculation procedure for the $1^2A'$ PEC, which is slightly different from the procedure described in section II. We noted that the H_1CBr angle values in the CASSCF partially optimized geometries of the $1^2A'$ state at R(C−Br) values larger than 3.3 Å were between 76° [at R(C−Br) = 3.3 Å] and 65° [at R(C−Br) = 5.0 Å]. We performed the B3LYP and MP2 PEC calculations for the $1^2A'$ state, and we noted that all the three HCBr angles in the B3LYP and MP2 partially optimized geometries at all the selected R(C−Br) values were larger than or close to 90°. The CASPT2//CASSCF Br-loss PEC for the $1^2A'$ state reported in the present paper was obtained based on the CASSCF partial geometry optimization calculations in which the H_1CBr angle values were fixed at the H_1CBr angle values (given in Table 3) in the MP2 partially optimized geometries at the respective R(C−Br) values.

The CH_3Br^+ systems of the four states at the R(C−Br) value of 5.0 Å will be called as asymptote products of Br-loss dissociation for the respective states in the following discussion. The CASPT2//CASSCF relative energies of the asymptote products of the four states to the $1^2A'$ reactant (the $1^2A'$ state at the CASSCF equilibrium geometry) are given in parentheses. In Table 3 are listed the CASPT2//CASSCF energies of the four states at selected R(C−Br) values, together with the charges on the Br atom [Q(Br)] and values of the principal geometric parameters in the CASSCF partially optimized geometries. The leading configurations in the CASSCF wave functions at selected R(C−Br) values are also given in Table 3.

As shown in Table 3, the Q(Br) values in the asymptote products of the $1^2A'$, $1^2A''$, $2^2A'$, and $2^2A''$ states are very small, which indicates that the products of Br-loss dissociation from the four states are the neutral Br atom plus the CH_3^+ ion in different states. In Table 4 are given the CASSCF geometries and CASPT2//CASSCF relative energies (T_0's) for the $1^1A_1'$ and $1^3A''$ states (the two lowest-lying states) of the CH_3^+ ion. The $1^2A'$, $1^2A''$, and $2^2A'$ asymptote products have similar CASPT2//CASSCF energies and the geometries of the CH_3 fragment in the asymptote products of the three states are similar to the CASSCF geometry of the $1^1A_1'$ state of the CH_3^+ ion (see Tables 3 and 4). We conclude that the $1^2A'$, $1^2A''$, and $2^2A'$ states of the CH_3Br^+ ion all correlate with the $1^1A_1'$ ground state of the CH_3^+ ion. On the basis of the CASPT2//CASSCF relative energy values given in Figure 2, the $2^2A''$ asymptote product is higher in energy than the $1^2A'$ asymptote product by 3.64 eV, which is close to the CASPT2//CASSCF T_0 value of 3.53 eV for the $1^3A''$ state of the CH_3^+ ion. The geometry of the CH_3 fragment in the $2^2A''$ asymptote product is close to the CASSCF geometry of the $1^3A''$ state of the CH_3^+ ion (see Tables 3 and 4). We conclude that the $2^2A''$ state of the CH_3Br^+ ion correlates with the $1^3A''$ state of the CH_3^+ ion.

Along the $1^2A'$, $1^2A''$, $2^2A'$, and $2^2A''$ Br-loss PECs, the energy increases monotonically with the R(C−Br) value. As shown in Table 3, the CASPT2//CASSCF energy of the $2^2A'$ state at R(C−Br) = 2.3 Å is lower than that at R(C−Br) = 2.63 Å (the C−Br bond length value in the CASSCF optimized geometry, see Table 1), which reminded us to reoptimize this C−Br bond length at the CASPT2 level (see section III.A). We assume that the appearance potential (AP) value for CH_3^+ ($1^1A_1'$) [AP for production of CH_3^+ ($1^1A_1'$) from the ground-state CH_3Br molecule] be equal to the sum of the experimental AIP value of 10.543 eV for the X^2E state[25] and the CASPT2//CASSCF relative energy value of 2.70 eV for the $1^2A'$ asymptote product (to the $1^2A'$ reactant), and the predicted AP value of 13.24 eV is higher than the experimental value of 12.80 eV [3] (reported in 1975) by 0.44 eV. We assume that the AP

TABLE 3: CASPT2//CASSCF Energies (E) at the Selected R(C−Br) Values for Br-Loss Dissociation from the $1^2A'$, $1^2A''$, $2^2A'$, and $2^2A''$ States, Together with Charge (Q) Values on the Br Atom, Values of Principal Geometric Parameters in the CASSCF Partially Optimized Geometries,[a] and the Leading Configurations in the CASSCF Wave Functions

R(C−Br) (Å)	E + 2643.0 (au)	Q(Br) (e)	R(C−H_2) (Å)	A(H_2CH_2') (deg)	D($H_2CH_1H_2'$) (deg)	R(C−H_1) (Å)	A(H_1CBr)[b] (deg)	leading configuration[c]
				$1^2A'$				
1.996	−1.07322	0.543	1.097	115.5	133.4	1.104		$(16a')^1$
3.0	−1.00964	0.238	1.096	120.0	171.6	1.096	92.4	$(16a')^1$
5.0	−0.97407	0.003	1.099	119.8	180.0	1.096	88.9	$(16a')^1$
				$1^2A''$				
1.998	−1.07312	0.542	1.101	112.0	131.8	1.094		$(6a'')^1$
3.0	−1.00976	0.239	1.096	119.6	171.5	1.095		$(6a'')^1$
5.0	−0.97469	0.003	1.099	120.0	179.9	1.099		$(6a'')^1$
				$2^2A'$				
2.3	−0.99332	0.269	1.098	119.3	162.9	1.097		$(16a')^1$
2.63	−0.98950	0.175	1.098	119.9	172.3	1.098		$(15a')^1$
3.0	−0.98253	0.175	1.099	120.0	177.8	1.099		$(15a')^1$
5.0	−0.96944	0.066	1.088	119.8	171.2	1.088		$(16a')^1$
				$2^2A''$				
2.065	−0.93973	0.217	1.185	74.6	84.4	1.096		$(5a'')^1$
3.0	−0.86535	0.090	1.189	62.0	76.6	1.096		$(5a'')^1$
5.0	−0.84024	0.001	1.200	55.5	67.2	1.100		$(5a'')^1$

[a] For notations, see Figure 1. [b] In the CASSCF partial geometry optimization calculations, the H_1CBr angle value was fixed at the angle value in the MP2 partially optimized geometry at each of the fixed R(C−Br) values. [c] The electronic configuration for the ground-state CH_3Br molecule is as follows: $...(5a'')^2(14a')^2(15a')^2(16a')^2(6a'')^2(17a')^0(18a')^0(19a')^0(7a'')^0$ in the C_s symmetry [$...(5e)^4(10a_1)^2(6e)^4(11a_1)^0(12a_1)^0(7e)^0$ in the C_{3v} symmetry].

TABLE 4: CASSCF Geometries and CASPT2//CASSCF Relative Energies (T_0) for the $1^1A'_1$ and $1^3A''$ States (the Two Lowest-Lying States) of the CH_3^+ Ion[a]

state	R(C−H_1) (Å)	R(C−H_2) (Å)	A(H_2CH_2') (deg)	D($H_2CH_1H_2'$) (deg)	T_0 (eV)
$1^1A'_1$[b]	1.097	1.100	119.8	180.0	0.0
$1^3A''$	1.096	1.197	56.0	68.1	3.53

[a] For notations, see Figure 1. [b] The ground state of the ion is $1^1A'_1$ in D_{3h} symmetry, and our calculations were performed within C_s symmetry.

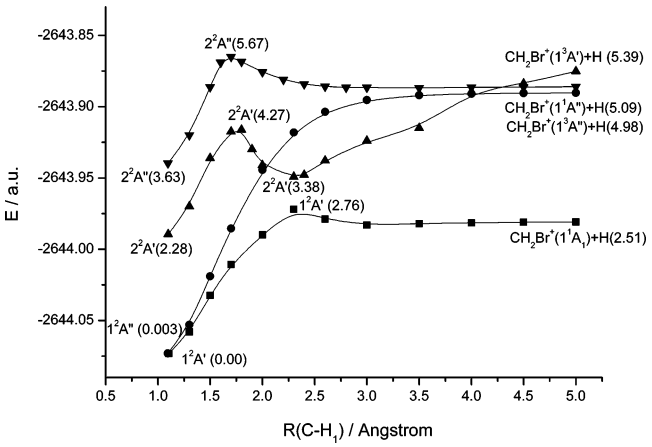

Figure 3. CASPT2//CASSCF potential energy curves (PECs) for H-loss dissociation from the $1^2A'$, $1^2A''$, $2^2A'$, and $2^2A''$ states. In parentheses are given the CASPT2//CASSCF relative energies (in eV) of the reactants, energy barriers, minima, and asymptote products along the PECs to the $1^2A'$ reactant.

value for $CH_3^+(1^3A'')$ be equal to the sum of the value of 10.543 eV (see above) and the CASPT2//CASSCF relative energy value (to the $1^2A'$ reactant) of the $2^2A''$ asymptote product, and the predicted AP value is 16.88 eV.

C. H-Loss Dissociation. In Figure 3 are given the CASPT2//CASSCF H-loss PECs for the $1^2A'$, $1^2A''$, $2^2A'$, and $2^2A''$ states of the CH_3Br^+ ion. The CH_3Br^+ systems of the four states at the R(C−H_1) value of 5.0 Å will be called as asymptote products of H-loss dissociation for the respective states in the following discussion. The CASPT2//CASSCF relative energies of the asymptote products of the four states to the $1^2A'$ reactant are given in parentheses. In Table 5 are listed the CASPT2//CASSCF energies of the four states at selected R(C−H_1) values, together with the charges on the H_1 atom [Q(H_1)] and values of the principal geometric parameters in the CASSCF partially optimized geometries. The leading configurations in the CASSCF wave functions at selected R(C−H_1) values are also given in Table 5.

As shown in Table 5, the Q(H_1) values are 0.000 e in the $1^2A'$, $1^2A''$, and $2^2A''$ asymptote products and small in the $2^2A'$ asymptote product, which indicates that the products of H-loss dissociation from the four states are the neutral H atom plus the CH_2Br^+ ion in different states. In Table 6 are given the CASSCF geometries and CASPT2//CASSCF relative energies (T_0's) for the 1^1A_1, $1^3A''$, $1^1A''$, and $1^3A'$ states (the four lowest-lying states) of the CH_2Br^+ ion. The $1^2A'$ ground state of the CH_3Br^+ ion correlates with the 1^1A_1 ground state of the CH_2Br^+ ion. As shown in Tables 5 and 6, the geometry of the CH_2Br fragment in the $1^2A'$ asymptote product is almost identical to the CASSCF geometry of the 1^1A_1 state of the CH_2Br^+ ion. On the basis of the CASPT2//CASSCF relative energy values given in Figure 3, the $1^2A''$ and $2^2A''$ asymptote products are higher in energy than the $1^2A'$ asymptote product by 2.47 and 2.58 eV, which are equal to the CASPT2//CASSCF T_0 values for the $1^3A''$ and $1^1A''$ states of the CH_2Br^+ ion, respectively (see Table 6). As shown in Tables 5 and 6, the geometries of the CH_2Br fragment in the $1^2A''$ and $2^2A''$ asymptote products are very close to the CASSCF geometries of the $1^3A''$ and $1^1A''$ states of the CH_2Br^+ ion, respectively. We conclude that the $1^2A''$ and $2^2A''$ states of the CH_3Br^+ ion correlate with the $1^3A''$ and $1^1A''$ states of the CH_2Br^+ ion, respectively.

As shown in Tables 5 and 6, the geometry of the CH_2Br fragment in the $2^2A'$ asymptote product [R(C−H_1) = 5.0 Å] is close to the CASSCF geometry of the $1^3A'$ state of the CH_2-

TABLE 5: CASPT2//CASSCF Energies (E) at the Selected R(C−H_1) Values for H-Loss Dissociation from the $1^2A'$, $1^2A''$, $2^2A'$, and $2^2A''$ States, Together with Charge (Q) Values on the Departing H_1 Atom and Values of Principal Geometric Parameters in the CASSCF Partially Optimized Geometries,[a] and the Leading Configurations in the CASSCF Wave Functions

R(C−H_1) (Å)	E + 2643.0 (au)	Q(H_1) (e)	R(C−H_2) (Å)	R(C−Br) (Å)	A(H_2CBr) (deg)	D(H_2CBrH_2') (deg)	R(H_1−Br) (Å)	leading configuration [b]
				$1^2A'$				
1.104	−1.07322	0.044	1.097	1.996	105.8	123.1		$(16a')^1$
2.3	−0.97194	0.106	1.084	1.849	119.7	174.3		$(16a')^1$
5.0	−0.98091	0.000	1.098	1.758	119.5	179.8		$(17a')^1$
				$1^2A''$				
1.094	−0.07312	0.035	1.101	1.998	103.7	117.2		$(6a'')^1$
2.3	−0.91802	0.053	1.099	1.939	109.5	134.2		$(6a'')^1$
5.0	−0.89034	0.000	1.100	1.906	111.5	141.2		$(6a'')^1$
				$2^2A'$				
1.098	−0.98950	0.110	1.098	2.630	92.2	120.0	2.889	$(15a')^1$
1.7	−0.91744	0.119	1.098	2.025	113.7	146.3	3.114	$(14a')^1$
1.8	−0.91625	−0.050	1.072	1.793	115.5	174.7	1.792	$(16a')^1$
1.9	−0.92990	−0.037	1.073	1.783	115.6	174.8	1.858	$(16a')^1$
2.0	−0.94100	−0.019	1.075	1.781	115.3	175.6	1.931	$(17a')^1$
2.3	−0.94915	0.156	1.074	1.869	116.1	177.1	2.074	$(17a')^1$
2.6	−0.93786	0.138	1.094	1.949	116.3	179.9	2.167	$(14a')^1$
3.0	−0.92395	0.124	1.093	1.958	115.7	172.4	2.234	$(14a')^1$
3.5	−0.91495	0.108	1.094	1.969	114.2	156.1	2.243	$(14a')^1(16a')^1(19a')^1$
5.0	−0.87507	0.019	1.093	2.041	110.1	144.3	3.284	$(14a')^1(16a')^1(19a')^1$
8.0	−0.87056	0.000	1.093	2.035	110.2	144.5	6.229	$(15a')^1(16a')^1(17a')^1$
				$2^2A''$				
1.096	−0.93973	0.067	1.185	2.065	115.8	84.6		$(5a'')^1$
1.6	−0.86894	0.153	1.187	2.049	117.6	88.7		$(5a'')^1$
1.7	−0.86493	0.037	1.096	2.114	102.9	137.1		$(14a')^1(6a'')^1(19a')^1$
5.0	−0.88600	0.000	1.097	1.934	112.1	148.4		$(16a')^1(17a')^1(6a'')^1$

[a] For notations, see Figure 1. [b] See footnote *c* for Table 3.

TABLE 6: CASSCF Geometries and CASPT2//CASSCF Relative Energies (T_0) for the 1^1A_1, $1^3A''$, $1^1A''$, and $1^3A'$ States (the Four Lowest-Lying States) of the CH_2Br^+ Ion

state	R(C−H) (Å)	R(C−Br) (Å)	A(HCBr) (deg)	D(HCBrH′) (deg)	T_0 (eV)
1^1A_1[a]	1.098	1.758	119.5	180.0	0.00
$1^3A''$	1.099	1.913	111.4	141.8	2.47
$1^1A''$	1.097	1.935	112.0	148.1	2.58
$1^3A'$	1.092	2.033	110.4	145.5	3.00

[a] The ground state of the ion is 1^1A_1 in C_{2v} symmetry, and our calculations were performed within C_s symmetry.

Br^+ ion. The $2^2A'$ asymptote product is higher in CASPT2//CASSCF energy than the $1^2A'$ asymptote product by 2.88 eV (see the relative energy values in Figure 3), which is 0.12 eV smaller than the CASPT2//CASSCF T_0 value of 3.00 eV for the $1^3A'$ state of the CH_2Br^+ ion. We continued the $2^2A'$ PEC calculations at the CASPT2//CASSCF level and we found that the $CH_3Br^+(2^2A')$ system at R(C−H_1) = 8.0 Å (it should be defined as the $2^2A'$ asymptote product of H-loss dissociation) be higher in CASPT2//CASSCF energy than the $1^2A'$ asymptote product by 3.00 eV, which is equal to the CASPT2//CASSCF T_0 value for the $1^3A'$ state of the CH_2Br^+ ion. On the basis of the CASSCF calculations, the Q(H_1) value in the new $2^2A'$ asymptote product is 0.000 e and the geometry of the CH_2Br fragment in the new $2^2A'$ asymptote product is almost identical to the CASSCF geometry of the $1^3A'$ state of the CH_2Br^+ ion. The present theoretical work predicts that the $2^2A'$ state of the CH_3Br^+ ion correlates with the dissociation limit of CH_2Br^+ ($1^3A'$) + H, though experimental workers[1,2] did not report H-loss dissociation from the A^2A_1 ($2^2A'$) state of the CH_3Br^+ ion. We will describe the calculated H-loss PEC of the $2^2A'$ state of CH_3Br^+ in the last paragraph of section III.C.

Along the $1^2A'$ H-loss PEC there is an energy barrier at R(C−H_1) ≈ 2.3 Å. The barrier is only 0.24 eV higher in CASPT2//CASSCF energy than the $1^2A'$ asymptote product and the CASPT2//CASSCF relative energy of the barrier to the $1^2A'$ reactant is 2.76 eV. Along the $1^2A''$ H-loss PEC, the energy increases monotonically with the R(C−H_1) value. By addtion of the experimental AIP value[25] (see above) for X^2E and the CASPT2//CASSCF relative energy value for the barrier along the $1^2A'$ H-loss PEC, the AP value for CH_2Br^+ (1^1A_1) is evaluated to be 13.30 eV, in reasonable agreement with the experimental value of 12.77 eV[2]. By adding the experimental AIP value[25] (see above) for X^2E and the CASPT2//CASSCF relative energy value of the $1^2A''$ asymptote product, the AP value for CH_2Br^+ ($1^3A''$) is evaluated to be 15.52 eV.

There is an energy barrier at R(C−H_1) ≈ 1.7 Å along the CASPT2//CASSCF H-loss PEC of the $2^2A''$ state, and it is 2.04, 0.58, and 5.67 eV higher than the $2^2A''$ reactant, the $2^2A''$ asymptote product, and the $1^2A'$ reactant, respectively. The CASSCF wave functions at large R(C−H_1) values along the $2^2A''$ PEC have shake-up ionization character.

There are an energy barrier at R(C−H_1) ≈ 1.8 Å and an energy minimum at R(C−H_1) ≈ 2.3 Å along the CASPT2//CASSCF H-loss PEC of the $2^2A'$ state, and the energy barrier and minimum are 1.99 and 1.10 eV higher than the $2^2A'$ reactant and 4.27 and 3.38 eV higher than the $1^2A'$ reactant, respectively. The H_1−Br distance values in the CASSCF partially optimized geometries of the $2^2A'$ state at selected R(C−H_1) values are also given in Table 5. The energy minimum along the $2^2A'$ H-loss PEC could be considered to correspond to an intermediate with a long C−H_1 bond distance (≈ 2.3 Å) and a long H_1−Br bond distance (2.074 Å), and this intermediate is much higher [25.4 kcal/mol (1.10 eV) at the CASPT2//CASSCF level] in energy than the $2^2A'$ reactant.

IV. Conclusions

In this section, we will first briefly summarize the present work on the CH_3Br^+ ion and then present a comprehensive review on the CAS calculation results for the CH_3X^+ (X = F, Cl, and Br) ions presented in our previous[13,14] and present papers.

The $1^2A'$, $1^2A''$, $2^2A'$, and $2^2A''$ states of the CH_3Br^+ ion have been studied by using the CASSCF and CASPT2 methods in conjunction with an ANO−RCC basis set. The $1^2A'$ state is predicted to be the ground state ($1^2A'$ and $1^2A''$ being the two Jahn−Teller component states of X^2E). The $2^2A'$ state is predicted to be a bound state. The CASPT2 T_0 value for $2^2A'$ is in reasonable agreement with the experimental value for the A^2A_1 state and the CASPT2 T_v' value for $2^2A'$ is very close to the experimental value for the A^2A_1 state. The CASPT2 T_v' value for $2^2A''$ (a Jahn−Teller component state of B^2E) is very close to the average of the experimental values for the B^2E state. Br-loss and H-loss dissociation PECs for the four C_s states of the CH_3Br^+ ion were calculated at the CASPT2//CASSCF level (the dissociation products and the features of the PECs to be mentioned in the comprehensive review below). The AP values for CH_3^+ ($1^1A_1'$), CH_3^+ ($1^3A''$), CH_2Br^+ (1^1A_1), and CH_2Br^+ ($1^3A''$) are evaluated.

On the basis of the previous CAS studies[13,14] on the CH_3F^+ and CH_3Cl^+ ions (using the ANO-L basis set in the calculations) and the present CAS study on the CH_3Br^+ ion (using the ANO−RCC basis set), we present a comprehensive review on the electronic states and the X-loss and H-loss dissociations of the CH_3X^+ (X = F, Cl, and Br) ions below.

A. Electronic States. The three lowest-lying C_{3v} states of the CH_3X^+ ions are X^2E, A^2A_1, and B^2E, and they become the five lowest-lying C_s states, $1^2A'$, $1^2A''$, $2^2A'$, $2^2A''$, and $3^2A'$. The $1^2A'$ and $1^2A''$ are considered as the two component states of the Jahn−Teller splitting in X^2E, and $2^2A''$ and $3^2A'$ are considered as the two component states of the Jahn−Teller splitting in B^2E. The two Jahn−Teller component states of a ^2E state have slightly different energies and the higher-energy component has a unique imaginary frequency corresponding to H-pivotal rotations.

For the CH_3F^+ ion the $1^2A''$ state is the ground state (the $1^2A'$ state being the higher-energy component), while for the CH_3Cl^+ and CH_3Br^+ ions the $1^2A'$ states are the ground states (the $1^2A''$ states being the higher-energy components). The $2^2A''$ state of CH_3F^+ lies below $3^2A'$. The $A^2A_1(2^2A')$ and B^2E ($2^2A''$ and $3^2A'$) states of CH_3F^+ are very close in energy at the geometry of the CH_3F molecule. We were not successful in calculating the $3^2A'$ states of CH_3Cl^+ and CH_3Br^+, and we would expect that the $3^2A'$ states of the two ions lie below the $2^2A''$ states since the $2^2A''$ states of the two ions are predicted to have the unique imaginary frequencies.

For the CH_3F^+ and CH_3Cl^+ ions, equilibrium geometries of the $2^2A'$ states were not found in the CASSCF geometry optimization calculations, in line with the suggestion based on experiment that the A^2A_1 states are repulsive. For the CH_3Br^+ ion, the equilibrium geometry of the $2^2A'$ state was found and it has a long C−Br bond length (2.630 and 2.315 Å predicted by the CASSCF and CASPT2 calculations, respectively). The previous PEC calculations for the CH_3Cl^+ ion[14] implied that an equilibrium geometry of the $2^2A'$ state of CH_3Cl^+ might be found in the PESs calculated at high levels (see the next paragraph).

B. X-Loss Dissociation. The CASPT2//CASSCF PECs were calculated for X-loss dissociation from the $1^2A''$, $1^2A'$, $2^2A'$, $2^2A''$, and $3^2A'$ states of the CH_3F^+ ion and the $1^2A'$, $1^2A''$, $2^2A'$, and $2^2A''$ states of the CH_3Cl^+ and CH_3Br^+ ions. The dissociation products from these states are the neutral X atom plus the CH_3^+ ion in different electronic states, and the electronic states of the CH_3^+ ion were determined by checking the relative energies and geometries of the asymptote products along the PECs. The PEC calculations for the X-loss dissociation indicate that the $1^2A'$, $1^2A''$, and $2^2A'$ states of the CH_3X^+ ions correlate with CH_3^+ (X^1A_1'); the $2^2A''$ states of the CH_3X^+ ions correlate with CH_3^+ ($1^3A''$); and the $3^2A'$ state of the CH_3F^+ ion correlates with CH_3^+ ($1^3A'$). The energy increases monotonically with the R(C−X) values along all the X-loss PECs except the $2^2A'$ X-loss PECs of CH_3F^+ and CH_3Cl^+.

C. H-Loss Dissociation. The CASPT2//CASSCF PECs were calculated for H-loss dissociation from the $1^2A'$, $1^2A''$, and $2^2A''$ states of the CH_3F^+ and CH_3Cl^+ ions and the $1^2A'$, $1^2A''$, $2^2A'$, and $2^2A''$ states of the CH_3Br^+ ion. The dissociation products from these states are the neutral H atom plus the CH_2X^+ ions in different electronic states, and the electronic states of the CH_2X^+ ions were determined by checking the relative energies and geometries of the asymptote products along the PECs. The PEC calculations for the H-loss dissociation indicate that the $1^2A'$, $1^2A''$, and $2^2A''$ states of the CH_3X^+ ions correlate with the X^1A_1, $1^3A''$, and $1^1A''$ states (the three lowest-lying states) of the CH_2X^+ ions, respectively. The energy increases monotonically with the $R(C-H_1)$ value along the $1^2A'$ and $1^2A''$ H-loss PECs (the energy increases almost monotonically with the $R(C-H_1)$ value along the $1^2A'$ H-loss PEC of CH_3Br^+). Along the $2^2A''$ H-loss PECs of the CH_3X^+ ions there are energy barriers and the CASSCF wave functions at large $R(C-H_1)$ values have shake-up ionization characters. The PEC calculations for the H-loss dissociation indicate that the $2^2A'$ state of the CH_3Br^+ ion correlates with the $1^3A'$ state of the CH_2Br^+ ion, which lies above the $1^1A''$ state. There are an energy barrier and a minimum along the $2^2A'$ H-loss PEC of the CH_3Br^+ ion. We were not successful in calculating the $2^2A'$ H-loss PECs for CH_3F^+ and CH_3Cl^+, and the preliminary calculations imply that the $2^2A'$ "PEC" of CH_3F^+ leads to the H^+ ion and that the $2^2A'$ "PEC" of CH_3Cl^+ does not directly lead to either the H atom or the H^+ ion.

Acknowledgment. This work was supported by the National Natural Science Foundation Committee of China (No. 20333050).

References and Notes

(1) Eland, J. H. D.; Frey, R.; Kuestler, A.; Schulte, H.; Brehm, B. *Int. J. Mass Spectrom. Ion Phys.* **1976**, *22*, 155.
(2) Lane, I. C.; Powis, I. *J. Phys. Chem.* **1993**, *97*, 5803.
(3) Tsai, B. P.; Baer, T.; Werner, A. S.; Lin, S. F. *J. Phys. Chem.* **1975**, *79*, 570.
(4) Brunetti, B.; Candori, P.; Andres, J. D.; Pirani, F.; Rosi, M.; Falcinelli, S.; Vecchiocattivi, F. *J. Phys. Chem. A* **1997**, *101*, 7505.
(5) Minchinton, A.; Cook, J. P. D.; Weigold, E.; Niessen, W. V. *Chem. Phys.* **1985**, *93*, 21.
(6) Olney, T. N.; Chan, W. F.; Cooper, G.; Brion, C. E.; Tan, K. H. *J. Electron Spectrosc. Relat. Phenom. Phys.* **1993**, *66*, 83.
(7) Utsunomiya, C.; Kobayashi, T.; Nagakura, S. *Bull. Chem. Soc. Jpn.* **1980**, *53*, 1216.
(8) Locht, R.; Leyh, B.; Dehareng, D.; Jochims, H. W.; Baumgärtel, H. *Chem. Phys.* **2005**, *317*, 87.
(9) Locht, R.; Leyh, B.; Jochims, H. W.; Baumgärtel, H. *Chem. Phys.* **2005**, *317*, 73.
(10) Locht, R.; Leyh, B.; Hoxha, A.; Dehareng, D.; Jochims, H. W.; Baumgärtel, H. *Chem. Phys.* **2000**, *257*, 283.
(11) Locht, R.; Leyh, B.; Hoxha, A.; Jochims, H. W.; Baumgärtel, H. *Chem. Phys.* **2001**, *272*, 259.
(12) Locht, R.; Leyh, B.; Hoxha, A.; Dehareng, D.; Jochims, H. W.; Baumgärtel, H. *Chem. Phys.* **2001**, *272*, 277.
(13) Xi, H.-W.; Huang, M.-B.; Chen, B.-Zh.; Li, W.-Z. *J. Phys. Chem. A* **2005**, *109*, 9149.

(14) Xi, H.-W.; Huang, M.-B.; Chen, B.-Zh.; Li, W.-Z. *J. Phys. Chem. A* **2005**, *109*, 4381.

(15) Roos, B. O. In *Ab Initio Methods in Quantum Chemistry*; Lawley, K. P., Ed.; Wiley: New York, 1987; Part 2.

(16) Andersson, K.; Malmqvist, P.-Å.; Roos, B. O.; Sadley, A. J.; Wolinski, K. *J. Phys. Chem.* **1990**, *94*, 5483.

(17) Andersson, K.; Malmqvist, P.-Å.; Roos, B. O. *J. Chem. Phys.* **1992**, *96*, 1218.

(18) Lugez, C. L.; Forney, D.; Jacox, M. E.; Irikura, K. K. *J. Chem. Phys.* **1997**, *106*, 489.

(19) Andersson, K.; Fülscher, M. P.; Lindh, R.; Malmqvist, P.-Å.; Olsen, J.; Sadlej, A. J.; Widmark, P.-O. *MOLCAS*, version 5.4. University of Lund: Lund, Sweden, 2002.

(20) Almlöf, J.; Taylor, P. R. *J. Chem. Phys.* **1987**, *86*, 4070.

(21) Widmark, P.-O.; Malmqvist, P.-Å.; Roos, B. O. *Theor. Chim. Acta* **1990**, *77*, 291.

(22) Widmark, P.-O.; Persson, B.-J.; Roos, B. O. *Theor. Chim. Acta* **1990**, *79*, 419.

(23) Roos, B. O.; Lindh, R.; Malmqvist, P.- Å.; Veryazov, V.; Widmark, P.-O. *J. Chem. Phys. A* **2004**, *108*, 2851.

(24) Kudchadker, S. A.; Kudchadker, A. P. *J. Phys. Chem. Ref. Data.* **1975**, *4*, 457.

(25) Karlsson, K.; Jadrny, R.; Mattsson, L.; Chau, F. T.; Siegbahn, K. *Phys. Scripta* **1977**, *16*, 225.

(26) Weitzel, K.-M.; Güthe, F.; Mähnert, J.; Locht, R.; Baumgärtel, H.; *Chem. Phys.* **1995**, *201*, 287.

(27) Orth, R. G.; Dunbar, R. C. *J. Chem. Phys.* **1978**, *68*, 3254.

(28) Won, D. S.; Kim, M. S.; Choe, J. C.; Ha, T.-K. *J. Chem. Phys.* **2001**, *115*, 5454.